Environmental Science & Technology

pubs.acs.org/est

Article

Mechanistic Insight into the Reproductive Toxicity of Trifloxystrobin in Male *Sprague–Dawley* Rats

Zheng Ma, Jing Chang,* Jianzhong Li, Bin Wan, and Huili Wang*

Cite This: *Environ. Sci. Technol.* 2024, 58, 22014−22026

Read Online

ACCESS | Metrics & More | Article Recommendations | Supporting Information

ABSTRACT: Previous studies have demonstrated the reproductive toxicity of trifluorostrobin (TRI) in male organisms. However, the underlying mechanisms of TRI responsible for testicular damage and hormonal disruption remain elusive. This study elucidated the male reproductive toxicity of TRI at the molecular level under environmentally relevant concentrations and its associations with gut microbiota dysbiosis. The rats were administered TRI (1.5, 15, and 75 mg/kg of body weight/day) continuously via gavage for 90 days. Exposure to 15 mg/kg (below the no-observed adverse effect level (NOAEL) of 30 mg/kg) and 75 mg/kg TRI damaged testicular tissue, reduced sperm count, and lowered serum hormone and total cholesterol levels. Transcriptomics analysis combined with molecular docking simulations and cell proliferation assays showed that exposure to TRI led to testicular damage by inhibiting the expression of cholesterol receptor genes, which, in turn, disrupted steroid hormone biosynthesis. Furthermore, exposure to TRI resulted in a marked decline in the relative abundance of the probiotic bacteria. Consistently, significant reductions in the relative abundance of short-chain fatty acids (SCFAs), retinoic acids, and steroid hormones in the gut were observed. Additionally, a significant correlation was observed between the relative abundance of *Parabacteroides* and serum testosterone levels, a vital biomarker for reproductive toxicity monitoring. These findings shed light on the mode of action of TRI-induced male reproductive toxicity and highlight the link between testicular injury and gut microbiota.

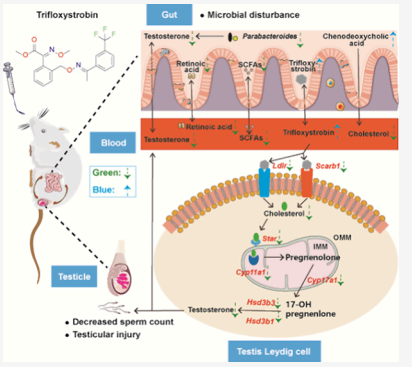

KEYWORDS: *Strobilurin fungicides, Testicular injury, Gut microbiota, Multiomics, Cell proliferation, Molecular docking*

1. INTRODUCTION

As one of the broad-spectrum strobilurin fungicides in terms of sales, trifloxystrobin (TRI) inhibits oxidative phosphorylation and ATP production by disrupting electron transfer and is extensively used in agriculture.[1,2] The widespread use of TRI has resulted in its leaching from soil into adjacent aquatic environments, posing risks to aquatic ecosystems and human health.[3] Studies have reported the presence of TRI in aquatic environments, with concentrations ranging from 0.41 to 170 μg/L in various countries.[4] TRI was also detected in terrestrial environment samples, exhibiting a concentration range of 0.81 to 1.8 μg/g.[5] TRI has been detected in the human serum with a maximum value of 0.015 μg/L.[6]

Reproductive toxicity refers to the harmful effects of a substance on any stage of the reproductive cycle, including impairments in reproductive functions and adverse effects on offspring.[7] Increasingly, research has demonstrated that TRI can induce reproductive toxicity in aquatic organisms, soil organisms, amphibians, and mammals.[8,9] Studies have specifically shown that environmentally relevant concentrations of TRI decreased the fertility (number of neonates) of *Daphnia magna*,[10] decreased the hatching rate of fertilized eggs of *Oryzias latipes*, and affected the expression of sex hormone genes in *Oryzias latipes* embryos.[11,12] In male zebrafish subjected to strobilurin fungicide exposure, a notable decline in testosterone concentration and gonadosomatic index was recorded, accompanied by evident histological alterations within the testes.[13] Furthermore, the standardized *Enchytraeid* reproduction assay revealed TRI as the most harmful pesticide (compared to azoxystrobin and pyraclostrobin), significantly reducing juvenile hatching in *Enchytraeus crypticus*.[14] A 90-day study in male dogs showed a 68% decrease in absolute testis weight, a 45% decrease in relative weight, moderate prostatic atrophy, and reduced sperm production.[15] Nevertheless, current research on elucidating the mechanism by which exposure to TRI impairs mammalian reproductive development remains insufficient. Molecular docking studies indicated that TRI could interact with the lactogen/cytokine receptor family, and exhibited an antagonistic conformation toward the steroid hormone receptor family.[16] Computational modeling by the US Environmental Protection Agency indicated that TRI exhibits significant androgen receptor (AR) activity and antagonistic effects.[17] The findings indicate that TRI emerges

Received: August 6, 2024
Revised: November 22, 2024
Accepted: November 22, 2024
Published: December 3, 2024

as a plausible endocrine disruptor, modulating the hypothalamic-pituitary−gonadal (HPG) axis and leading to sex hormone imbalances and testicular damage through altered gene expression.

Recent research has amassed compelling evidence suggesting that contact with pesticides can adversely affect the host's gut microbiota, contributing to metabolic disorders.[18−20] The intestinal flora exerts an influence on the synthesis of leptin and catecholamines through metabolites, thereby modulating the HPG axis to impact reproductive development.[21] Research demonstrated that the intestinal microbiota assume a pivotal role in regulating the metabolism of androgens. The gut microbiota can efficiently deglucuronidate intestinal glucuronidated testosterone and dihydrotestosterone.[22] This process leads to the accumulation of most androgens in the distal gut and may even breach the blood testis barrier to regulate spermatogenesis.[23] Emerging research has revealed that strobilurin fungicides disrupt the proliferation of the intestinal microbiota, subsequently eliciting a perturbation in the gut microbiome equilibrium.[24] However, the potential for TRI to adversely affect male reproduction via alterations in the gut microbiota remains unelucidated.

Despite increasing research, TRI's reproductive toxicity mechanisms remain elusive. This study bridges gaps in TRI's mammalian toxicology, investigating the potential association between gut microbiota disruption and reproductive harm. It offers fresh perspectives on TRI's reproductive toxicity mechanisms.

2. MATERIALS AND METHODS

2.1. Materials and Reagents. Trifloxystrobin (TRI, pureness >97%) was obtained from Jiangsu Changqing Agrochemical Company Limited (Jiangsu, China). TRNzol universal reagent was procured from Beijing Tiangen Biotech Company Limited (Beijing, China). HPLC-compliant solutions, including acetonitrile and methanol, were obtained from Thermo Fisher Technology Company Limited (Beijing, China).

2.2. Animals and Experimental Design. Specific pathogen-free (SPF) male *Sprague−Dawley* (SD) rats (average body weight 166.58 ± 5.34 g) were obtained from Beijing Si Pei Fu Biotechnology Company Limited. Details of feeding conditions are provided in Text S1.

After a 7-day acclimatization period, 40 rats were randomized into 4 groups (n = 10): a control group (administered corn oil) and three treatment groups receiving low (TRI-L, 1.5 mg/kg body weight/day), medium (TRI-M, 15 mg/kg body weight/day), and high (TRI-H, 75 mg/kg body weight/day) doses of TRI dissolved in corn oil, respectively. The dosage of 1.5 mg/kg was comparable in magnitude to the residual concentrations observed in soil, ranging from 0.81 to 1.8 mg/kg.[5] Additionally, the dosage of 15 mg/kg was half of the NOAEL (30 mg/kg) established in rats.[15] The lowest observable adverse effect level (LOAEL) of TRI was 73 mg/kg.[15] Based on prior studies, concentrations exceeding 73 mg/kg were deemed the "high dosage" of TRI. TRI was orally administered to rats daily via gavage for 90 days, adhering to the organization for economic cooperation and development standard (test No. 408).[25]

Weekly body weights were recorded. Upon completion, serum, brain, liver, testis, epididymis, and cecum were harvested and stored at −80 °C for TRI concentration analysis. Detailed measurement methods and results are shown in Text S2, Table S1−S3, and Figure S1, respectively. The limit of quantification (LOQ) of TRI was 5 μg/L. The left gonads were fixed in 10% neutral buffered formalin for histopathological analysis, and a serum aliquot was stored at −80 °C for hormone and biochemical analysis. The animal use protocols listed above have been reviewed and approved by the Animal Ethics and Welfare Committee of the Research Center for Eco-Environmental Sciences, Chinese Academy of Sciences (AEWC-RCEES-2023044).

2.3. Sperm Quantity and Motility Analysis. Sperm quantity and motility were quantified following a published procedure.[26] To assess sperm characteristics, the left caudal epididymis was employed. After the excision of residual adipose tissue, it was immersed in a 37 °C preheated normal saline (20 mL) culture dish. Fragmentation facilitated sperm release, followed by incubation at 37 °C for 10 min. Afterward, the sperm suspension was diluted and added to a blood cell counting plate for sperm counting under a microscope (Olympus BX53F2, Japan). At the same time, cell smears of semen samples were prepared, and about 200 sperm were randomly observed and recorded. Sperm motility is divided into four levels: A (fast forward), B (slow or sluggish forward), C (nonforward), and D (immobile). Sperm motility percentage is calculated as the sum of the number of classes A and B divided by the total number of observed sperm.

2.4. Histological Analysis of Testis. The left testes underwent 24 h fixation at ambient temperature and dehydration through a series of ethanol and xylene solutions. Subsequently, the tissues were embedded in paraffin wax. These embedded blocks were sectioned into 4 μm-thick slices, stained with hematoxylin-eosin (HE), and observed to record the status of 400 seminiferous tubules per animal using a light microscope (Olympus BX53F2, Japan).

A quantitative assessment of seminiferous tubules was performed, categorizing them as either normal (featuring concentric, organized germ cell layers in the seminiferous epithelium) or abnormal (marked by reduced sperm quantity, appearance of sloughed germ cells within the tubular lumen, and Sertoli cell displacement).[27]

2.5. Measurement of Serum Hormonal Concentrations and Analysis of Serum Biochemistry. The concentrations of estradiol (E_2) and luteinizing hormone (LH) in rat serum were quantified utilizing dedicated enzyme-linked immunosorbent assay (ELISA) kits (Shanghai Enzyme-linked Biotechnology Company Limited. Shanghai, China, code no. ml002871, ml002860). The levels of testosterone (T) and progesterone were determined by high-performance liquid chromatography coupled with tandem mass spectrometry (HPLC-MS-MS). The serum extraction method and the extraction method validation outcomes are presented in Text S3 and Tables S3−4. Instrumental and chromatographic conditions are listed in Table S5. The limit of quantification (LOQ) of T and progesterone was 0.1 μg/L. Concurrently, the protein concentrations within the serum samples were quantified using a bicinchoninic acid (BCA) assay kit (Shanghai Beyotime Biotechnology Company Limited. Shanghai, China, Code#, P0010S) to standardize hormone levels. The experimental procedures are rigorously executed in adherence to the manufacturer's instructions provided with the kit.

Clinical variables including albumin II (ALB), alkaline phosphatase (ALP), alanine aminotransferase (ALT), aspartate aminotransferase (AST), cholinesterase (CHE), creatinine

https://doi.org/10.1021/acs.est.4c08168
Environ. Sci. Technol. 2024, 58, 22014−22026

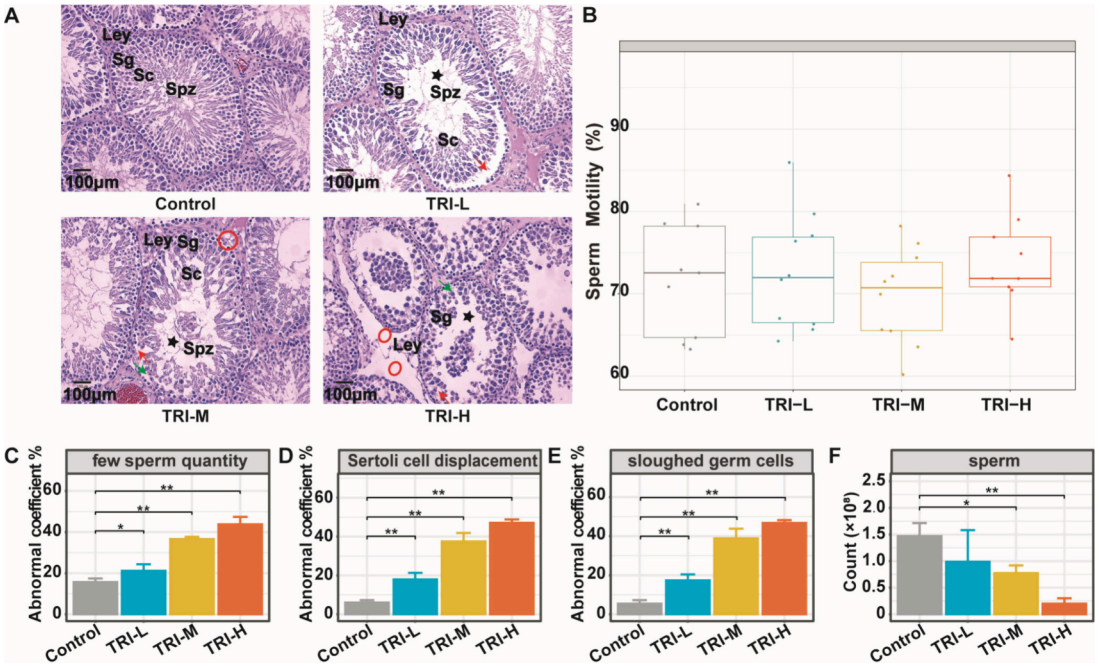

Figure 1. Effects of 1.5 mg/kg (TRI-L), 15 mg/kg (TRI-M), and 75 mg/kg (TRI-H) TRI exposure on testis histology, epididymal sperm motility, and quantity in SD rats. (A) The histopathological changes of testes. Ley (Leydig cells), Sg (spermatogonia cells), Sc (Sertoli cells), Spz (sperm), red arrows indicate vacuolation, black five-pointed star indicates few sperm quantity, green arrow indicates a decrease in shedding and a disordered arrangement of spermatogenic cells, red ovals indicate reduced Leydig cells. Abnormal coefficients in 400 randomly seminiferous tubules/animal, including (C) few sperm quantity, (D) Sertoli cell displacement, and (E) occurrences of sloughed germ cells. Epididymal sperm motility (B) and quantity (F). Data are expressed as mean ± SD (n = 5). Compared with the control group, * represented $p < 0.05$, and ** indicated $p < 0.01$.

serum (CREA-S), globulin II (Glo), glucose (Glu-G), triglyceride (TG), total cholesterol (TC), total protein II (TP), and urea (UREA) in rat serum were analyzed using a Hitachi 7080 automatic biochemistry analyzer (Hitachi, Japan) by biochemical colorimetry.[28]

2.6. Transcriptome Analysis of Rat Testis. Total RNA was extracted from 50 mg of rat testis samples (n = 5/group) in the control, TRI-M, and TRI-H treatments using TRIzol reagent. RNA quality was assessed using a Nanophotometer (IMPLEN, CA, USA) by measuring the 260/280 nm absorbance ratio to ensure purity and integrity. The processes of RNA sequencing and quality assurance measures were carried out by Beijing Novogene Company Limited (Beijing, China).

The analysis of transcriptomic data and reverse transcription-quantitative polymerase chain reaction (RT-qPCR) validation were conducted following a modified version of a previously published procedure.[29] Comprehensive descriptions have been presented in Text S4−S5 and Table S6. The raw transcriptome sequencing data have been archived in the NCBI databases, accessible via accession number PRJNA1123163 (to be released).

2.7. Gut Microbiota Analysis. Genomic DNA was extracted from cecal fecal samples in the control, TRI-M, and TRI-H groups utilizing the Stool Genomic DNA Extraction Kit (Beijing Solarbio Science & Technology Company Limited. Beijing, China, Code#, D2700) following the manufacturer's guidelines. Bacterial genomic DNA from rat cecal contents (n = 5/group) was sequenced by Beijing Novogene Company Limited (Beijing, China).

The analysis of gut microbiome data was performed using a modified version of a previously established protocol.[30] Detailed descriptions are provided in Text S6. Raw bacterial 16S rDNA gene sequencing data have been archived in NCBI databases under accession number PRJNA1126853 (to be released).

2.8. Metabolomics Analysis. Two hundred milligrams of cecum fecal samples (n = 5/group) from the control, TRI-L, TRI-M, and TRI-H exposure groups were used for nontargeted metabolomics analysis. The ultimate 3000 ultrahigh-performance liquid chromatography coupled with Q Exactive Focus Orbitrap mass spectrometer (UPLC-QE, Thermo Scientific, USA) was used for metabolomics analysis, as detailed by Chang et al. (2023).[29] Comprehensive descriptions of both data analysis methodologies and instrumentation protocols are furnished in Text S7 and Table S7. Relative quantification of several significantly changed metabolites related to SCFAs, bile acids, and steroid hormone synthesis was applied to confirm the metabolomics data. The relative quantification method and target metabolites information were described in Text S8 and Table S8 respectively.

2.9. Cellular Proliferation Assessment. The lymph node carcinoma of the prostate (LNCaP) cell line was acquired from the esteemed Chinese Academy of Medical Sciences (Beijing, China). When assessing LNCaP proliferation after chemical exposure, we referred to the previously described protocols.[31,32] The detailed cell culture method and mode of TRI exposure are provided in Text S9.

2.10. Yeast Two-Hybrid Assay. Recombinant androgen receptor gene two-hybrid yeast kindly was provided by Ma Mei professor at the Research Center for Eco-Environmental Sciences, Chinese Academy of Sciences (Beijing, China). The yeast assay was carried out as described by Li et al. (2008).[33] The detailed yeast cell culture method and mode of TRI exposure are provided in Text S10.

https://doi.org/10.1021/acs.est.4c08168
Environ. Sci. Technol. 2024, 58, 22014−22026

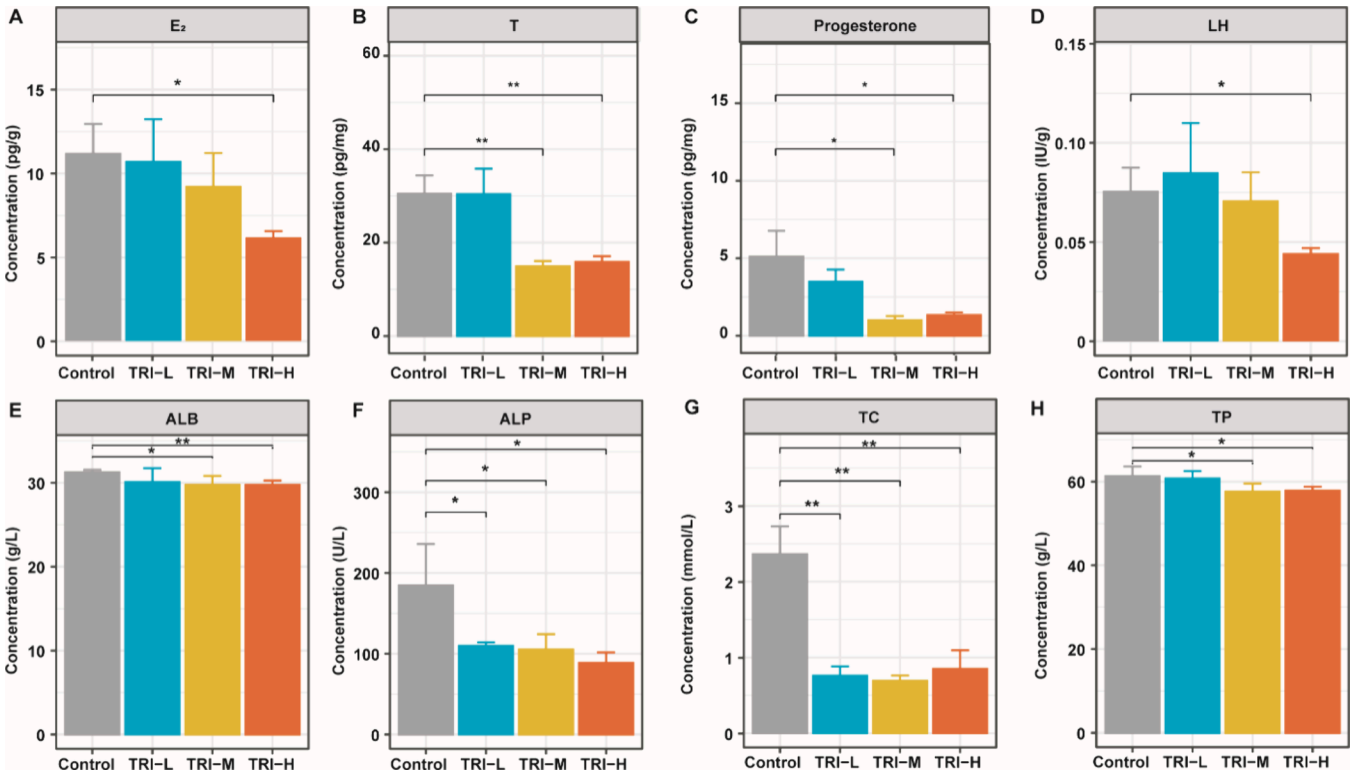

Figure 2. Effects of TRI exposure on hormone levels and serum biochemistry in SD rats. The levels of (A) E_2, and (D) luteinizing hormone (LH) in rat serum were measured by ELISA in the control, 1.5 mg/kg (TRI-L), 15 mg/kg (TRI-M), and 75 mg/kg (TRI-H) exposure groups. The levels of (B) T and (C) Progesterone in rat serum were measured by HPLC-MS-MS. The levels of (E) albumin II (ALB), (F) alkaline phosphatase (ALP), (G) total cholesterol (TC), and (H) total protein II (TP) in rat serum were measured by automatic biochemistry analyzer. Data are expressed as mean ± SD (n = 5). Compared with the control group, * represented $p < 0.05$, and ** indicated $p < 0.01$.

2.11. Molecular Interaction Simulation through Docking Analysis. The crystal structure of the rat AR ligand binding domain complex with an inhibitor (PDB ID: 3G0W) was downloaded from the RCSB Protein Data Bank. The initial models of the rat low-density lipoprotein receptor (LDLR) and scavenger receptor class B member 1 (SCARB1) were constructed by leveraging homology modeling techniques on the Swiss Model platform.[34] Specifically, the human LDLR crystal structure (PDB ID: 3M0C) was used to model rat LDLR, while the AlphaFold model (P97943.1.A) was used for constructing rat SCARB1. The comprehensive data analysis methodologies and their corresponding outcomes are presented in Text S11. Furthermore, a visual representation of the 2D ligand−receptor interaction diagram has been crafted for the ligand−receptor complex, offering a clear and intuitive understanding of the binding interface.

2.12. Statistical Analyses. The results are comprehensively presented as mean values accompanied by standard deviations (SD). Statistical differences were assessed using unpaired two-tailed Student's t-test for comparisons between two groups or one-way analysis of variance (ANOVA) for multiple comparisons with the least significant difference (LSD) method. Before performing ANOVA, the assumptions of normality and homogeneity of variances were rigorously assessed. Statistical significance was considered to be achieved when the p-value <0.05. The data visualizations were crafted utilizing the R Studio (version 4.2.1).

3. RESULTS AND DISCUSSION

3.1. Quantification of TRI Concentrations in Rat Serum and Tissues. The concentrations of TRI residues in the serum, brain, testis, liver, and cecum of rats after different dosages of TRI (1.5, 15, and 75 mg/kg) exposure were 2.87−4.41 μg/L, 0.14−0.21 μg/g, 0.11−0.44 μg/g, 0.28−0.64 μg/g, and 0.44−1.17 μg/g, respectively (Figure S1). After TRI exposure, TRI preferred to be accumulated in the serum, liver, and cecum. In the present study, blood was collected 24 h after the last gavage treatment, and the highest residual concentration of TRI was found in the serum. This observation aligns with prior research, suggesting that the peak serum concentration occurs within a time frame of 12 to 48 h.[15] This finding can be attributed to the long half-life of TRI in blood (25−41 h).[15] Furthermore, the data implies that upon achieving stable concentration, TRI exhibits over 95% binding affinity to plasma proteins.[35,36] This high binding capacity may also contribute to the elevated concentration of TRI in the serum. Remarkably, the TRI concentrations in serum, liver, and cecum observed in this study aligned with environmental levels (0.41−170 μg/L or 0.81−1.8 μg/g).[3−5] In conclusion, continuous TRI exposure resulted in its accumulation in the testes and serum, potentially contributing to male reproductive toxicity.

3.2. Effects of TRI Exposure on Testicular Histology and Sperm Quantity. Administration of TRI-H led to a marked decline in body weight among rats after 20 days of intragastric dosing, as compared with the control group (Figure S2). Sperm motility analysis showed no significant difference in advanced motility between the TRI-treated and

https://doi.org/10.1021/acs.est.4c08168
Environ. Sci. Technol. 2024, 58, 22014−22026

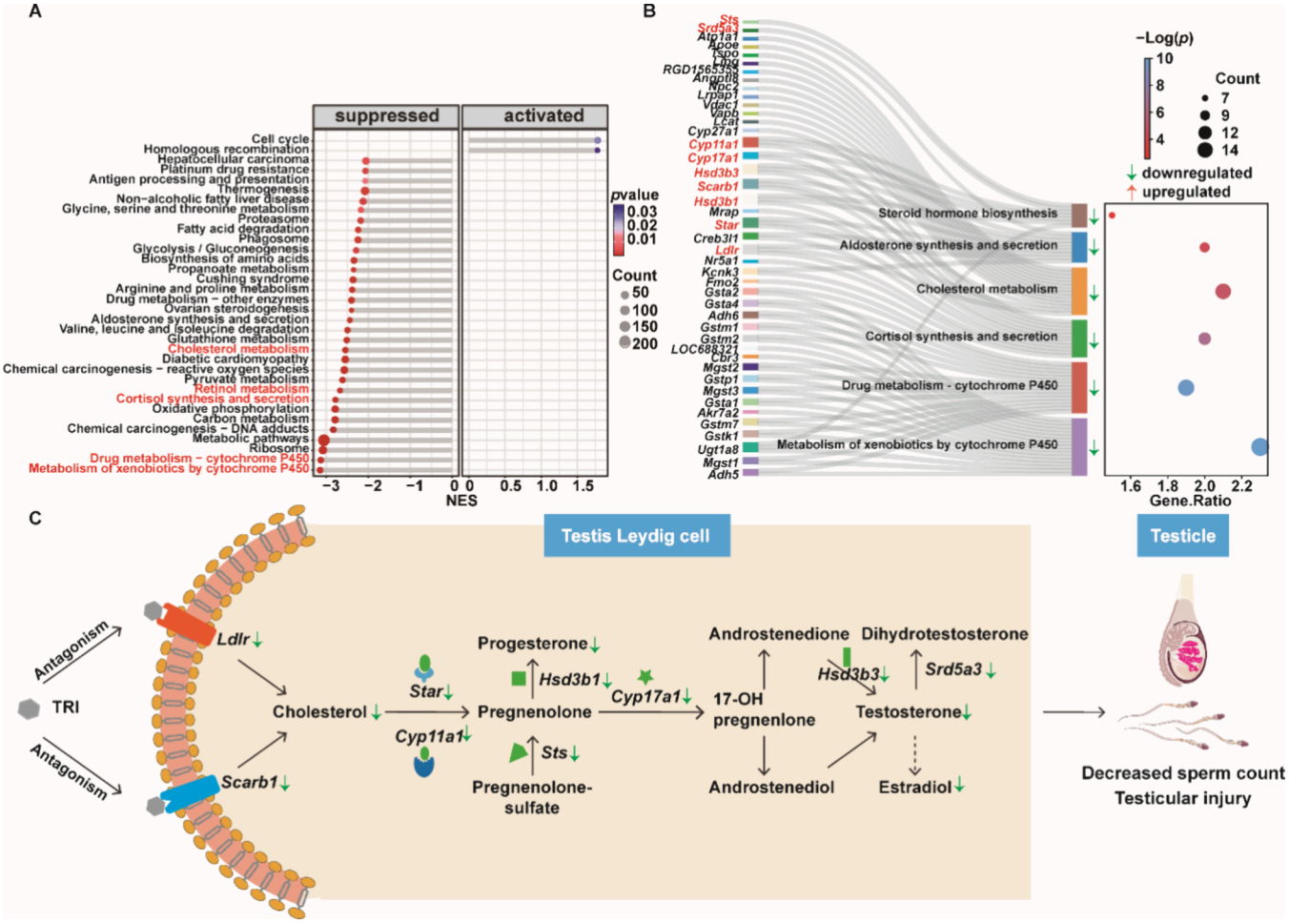

Figure 3. Transcriptomic analysis of the TRI-exposed rat testis. (A) The KEGG pathways significantly enriched by GSEA in the 75 mg/kg (TRI-H) exposure groups compared with the control group, the size of the bubble indicates the number of DEGs, and the color of the bubble indicates the size of *p*-value (FDR-adjusted $p \leq 0.05$). (B) Sankey plot showcasing DEGs were involved in critical focus enriched pathways obtained via GSEA-KEGG analysis in the TRI-H exposure groups compared with the control group, the red arrow means the path is upregulated while green is downregulated, and the size of the bubble indicates the number of DEGs (FDR-adjusted $p \leq 0.05$). (C) Diagram of the steroidogenic pathway, the green arrow means the gene expression or hormone levels are declining. Abbreviations: *Ldlr*, low-density lipoprotein receptor; *Scarb1*, scavenger receptor class B member 1; *Star*, steroidogenic acute regulatory protein; *Cyp11a1*, cytochrome P450 family 11 subfamily A polypeptide 1; *Sts*, steroid sulfatase; *Cyp17a1*, cytochrome P450 family 17 subfamily A polypeptide 1; *Hsd3b1*, hydroxy-delta-5-steroid dehydrogenase 3 beta- and steroid delta-isomerase 1; *Hsd3b3*, hydroxy-delta-5-steroid dehydrogenase 3 beta- and steroid delta-isomerase 3; *Srd5a3*, steroid 5 alpha-reductase 3.

control groups (ANOVA; $F = 0.72$; $p = 0.55$) (Figure 1B). Sperm motility is primarily influenced by its structural and functional integrity. Prolonged exposure to toxic chemicals can lead to a reduction in sperm count; however, sperm motility may remain unaffected, depending on individual variability.[37] Control rats displayed normal Leydig cell morphology, organized spermatogenic cells, typical Sertoli cells, intact seminiferous tubule membranes, abundant spermatozoa, and no spermatogonia detachment (Figure 1A). Exposure to TRI significantly increased the percentage of abnormalities of the seminiferous tubules, including few sperm quantity (ANOVA; $F = 87.35$; $p < 0.0001$) (Figure 1C), Sertoli cell displacement (ANOVA; $F = 150.70$; $p < 0.0001$) (Figure 1D), and the occurrence of sloughed germ cells (ANOVA; $F = 142.90$; $p < 0.0001$) (Figure 1E). Exposure to TRI-M and TRI-H groups reduced rat epididymal sperm counts to 52.84% and 16.19% of the control group, respectively (ANOVA; $F = 10.21$; $p = 0.0013$) (Figure 1F). This result is consistent with that observed through HE staining of the testis tissue (Figure 1A). These results indicated that TRI exposed to rats at levels lower than NOAEL (30 mg/kg) also resulted in testicular damage and reduced sperm counts. Previous studies have also shown that exposure to TRI could damage the testicles and epididymis with a secondary moderate or marked reduction of spermatozoa.[11,15,24] This study detected TRI-induced male reproductive toxicity in rats at a lower dose (15 mg/kg) than previous feed exposure studies, likely due to the precise dosing via gavage.[38] Normal maturation of spermatozoa depends on the proper development of spermatogenic cells in the testis.[39] The decrease in the sperm count after exposure to TRI was directly related to the abnormal development of spermatogonia cells.

3.3. Effects of TRI Exposure on Hormonal Profiles and Serum Biochemical Parameters. The maintenance of steroid hormone concentrations is essential for the progression of reproductive system development. In this study, exposure to TRI-H group reduced rat serum E_2 and LH levels to 54.64% and 62.38% of untreated group, respectively (ANOVA; $F =$

https://doi.org/10.1021/acs.est.4c08168
Environ. Sci. Technol. 2024, 58, 22014−22026

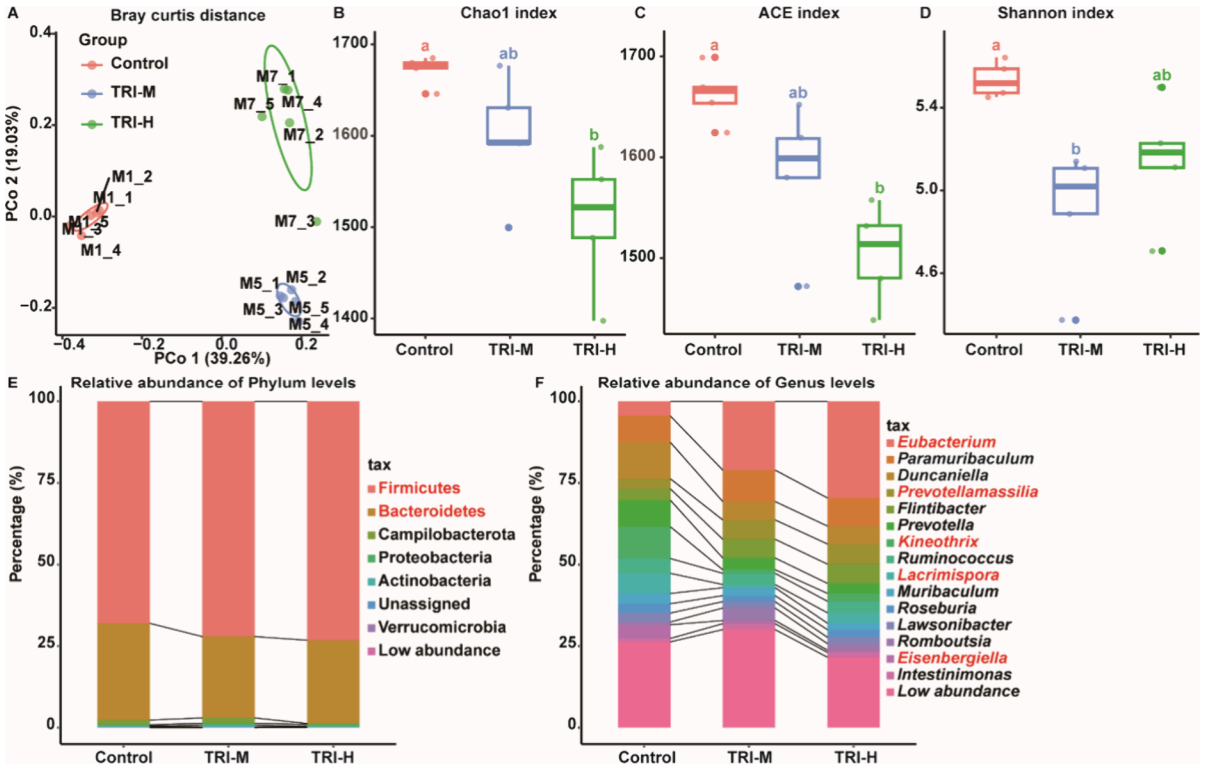

Figure 4. Effects of TRI exposure on gut microbiota composition of rats. β-diversity analysis:(A) Bray−Curtis distance. α-diversity analysis: (B) Chao1 index, (C) ACE index, and (D) Shannon index. Composition of microbial community and the main microbiota at (E) phylum and (F) genus level in the control, 15 mg/kg (TRI-M), and 75 mg/kg TRI (TRI-H) exposure groups. Statistical significance was determined by one-way ANOVA and the LSD posthoc test. Data are expressed as mean ± SD (n = 5). Bars with different letters represent a significant difference between groups ($p < 0.05$).

4.31, and 3.27; p = 0.0383, and 0.0401) (Figure 2A, and 2D), while T and progesterone levels were significantly decremented to 52.12% and 30.42% of untreated group, respectively (ANOVA; F = 5.65, and 3.68; p = 0.0030, and 0.0216) (Figure 2B, and 2C). Exposure to the TRI-M group also reduced rat serum T and progesterone levels to 49.12% and 30.93% of the untreated group, respectively ($p < 0.05$) (Figure 2B, and 2C). T production in Leydig cells is regulated by LH, which influences Sertoli cell activity and supports spermatogenesis in seminiferous tubules.[40,41] Thus, the decreased levels of T, E_2, progesterone, and LH further confirm the disruption of the hormones associated with TRI-induced testicular damage. Further investigation is necessary to determine the specific mechanisms of sex hormone disruption.

Serum biochemical indicators are important biomarkers to reflect the homeostasis and disease status of the body.[42] Compared with the control group, notable reductions were observed in ALB, ALP, TC, and TP levels within the TRI-M and TRI-H samples (ANOVA; F = 3.27, 9.00, 8.57, and 5.48; p = 0.0488, 0.0010, 0.0013, and 0.0096) (Figure 2E-H), while CREA-S and UREA levels were significantly elevated in the TRI-H samples (ANOVA; F = 3.31, and 8.00; p = 0.0493, and 0.0024) (Figure S3D, and S3H). Changes in these indicators indicate that exposure to TRI impairs normal functions of the liver and kidneys. It is important to note that cholesterol is a crucial raw material for the production of mammalian steroid hormones and other physiologically active substances.[43] The drop in sex hormone levels may be induced by the decrease in total cholesterol levels found in the serum. However, body cholesterol levels are regulated by the balance of dietary intake, endogenous production, and elimination of cholesterol and bile acids.[44]

3.4. Transcriptomic Analysis on the TRI-Exposed Rat Testis. A combined transcriptome and metabolic profiling analysis reveals key genes, metabolites, and regulatory pathways that enhance our understanding of pollutant toxicity mechanisms.[45] Therefore, the 15 mg/kg (TRI-M) and 75 mg/kg (TRI-H) exposed groups, which caused significant damage to rat testes, were selected for transcriptomic analysis. The differentially expressed genes (DEGs) in the TRI-M and TRI-H groups were 123 (46 downregulated and 77 upregulated) and 1052 (478 downregulated and 574 upregulated), respectively (Figure S4A, B). The number of DEGs found in transcriptomics increased with increased TRI exposure doses.

An investigation into the Gene Ontology-biological process (GO-BP) revealed that the top 30 terms were consistently modulated by two treatment groups (Figure S4C). Notably enriched GO terms in both TRI-treatment groups, such as ″reproductive system development (GO: 0061458)″, ″reproductive structure development (GO: 0048608)″, and ″gonad development (GO: 0008406)″, were strongly linked to testicular development and sperm maturation. More DEGs were enriched in these GO pathways in the TRI-H group than in the TRI-M group, suggesting a dose-dependent relationship.

GSEA-KEGG pathway analysis indicated that the TRI-M group activated one of the top 11 pathways and inhibited 10 (Figure S4D), while the TRI-H group activated two of the top 34 pathways and inhibited 32 (Figure 3A). Pathways suppressed after TRI-H exposure included “metabolism of xenobiotics by cytochrome P450 (KO: 00980)”, “drug

https://doi.org/10.1021/acs.est.4c08168
Environ. Sci. Technol. 2024, 58, 22014−22026

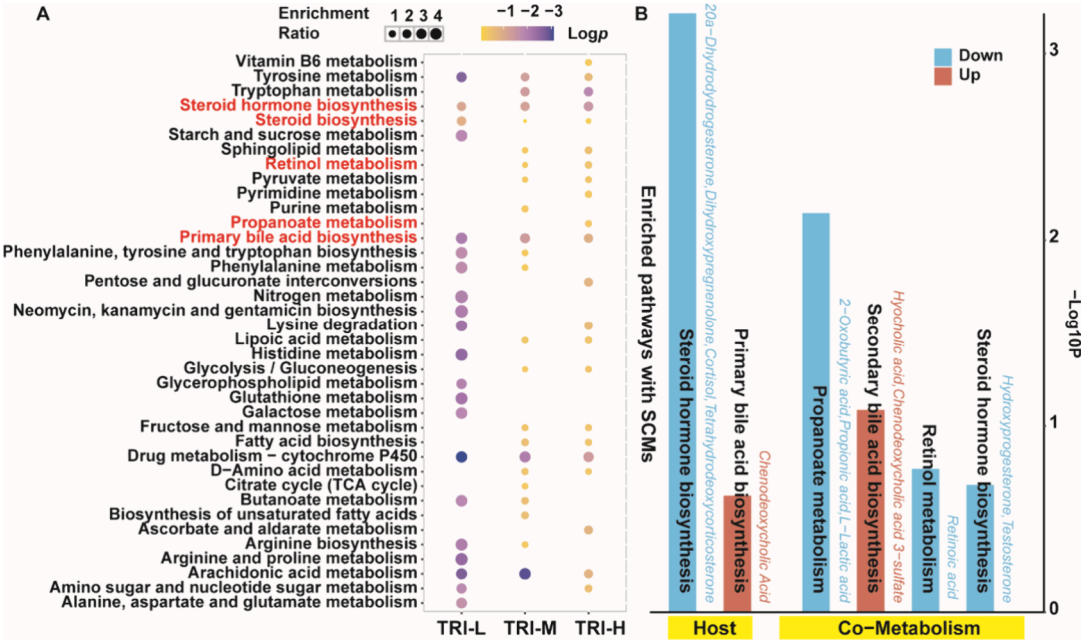

Figure 5. Metabolomics analysis on the TRI-exposed rat cecum fecal. (A) The KEGG metabolic pathway in the 1.5 mg/kg (TRI-L), 15 mg/kg (TRI-M), and 75 mg/kg TRI (TRI-H) exposure groups by metabolomics analysis, the size of the bubble indicates the proportion of metabolites occupying the entire pathways, the color represents the *p*-values. (B) Enrichment bar plot showcasing SCMs were involved in critical focus enriched pathways obtained via deep MetOrigin analysis, the red color means the pathways and SCMs are upregulated while blue is downregulated, the Host indicates SCMs from host, the Co-Metabolism indicates SCMs from bacteria and host.

metabolism-cytochrome P450 (KO: 00982)", "cortisol synthesis and secretion (KO: 04927)", "retinol metabolism (KO: 00830)", and "cholesterol metabolism (KO: 04979)". These inhibited pathways were consistent with the decrease in serum levels of total cholesterol and sex hormones following exposure to the TRI-H group. After TRI exposure, six pathways related to testicular development and sex hormone levels were significantly inhibited, with key DEGs (*Ldlr*, *Scarb1*, *Star*, *Cyp11a1*, *Sts*, *Cyp17a1*, *Hsd3b1*, *Hsd3b3*, and *Srd5a3*) significantly downregulated (Figure 3B). To validate the transcriptomic results, the expression of 10 DEGs (*Scarb1*, *Star*, *Cyp11a1*, *Cyp17a1*, *Hsd3b1*, *Hsd3b3*, *Dnai1*, *Tex47*, *Rb1cc1*, and *Cylc2*) was confirmed by RT-qPCR. The results of RT-qPCR validation were consistent with the transcriptomic results (Figure S5).

Most steroid-producing cholesterol comes from circulating lipoproteins, primarily low-density lipoproteins (LDLs) and high-density lipoproteins (HDLs).[43] In humans, steroid cholesterol synthesis primarily occurs via *Ldlr*-mediated LDL absorption, while rodents favor *Scarb1*-mediated HDL absorption.[46] Thus, TRI may lower *Ldlr* and *Scarb1* expression by antagonizing cholesterol receptors, impairing cholesterol absorption and metabolism as well as steroid hormone biosynthesis. Reduced free cholesterol uptake limits precursors for steroid hormone biosynthesis, which is transported by the steroidogenic acute regulatory protein (*Star*) across the inner mitochondrial membrane.[47] This led to the downregulation of cytochrome P450 family 11 and 17 subfamilies A polypeptide 1 (*Cyp11a1*, *Cyp17a1*), hydroxysteroid dehydrogenases (*Hsd3b1*, *Hsd3b3*), and 5α-reductase (*Srd5a3*) involved in sex hormone synthesis in Leydig cells, resulting in reduced serum testosterone and estradiol levels.[46,48] In conclusion, the antagonistic effect of TRI on cholesterol receptors ultimately led to disturbed cholesterol and hormone levels, resulting in testicular damage (Figure 3C).

3.5. Effects of TRI Exposure on the Composition and Function of the Gut Microbiota. Recent discoveries indicate that gut microbiota disruptions can cause pathological changes in the male reproductive system, including vacuole formation in the testes and seminiferous tubules and reduced sperm count.[19,30,49] Therefore, the effects of 15 mg/kg (TRI-M) and 75 mg/kg (TRI-H) TRI on the gut microbiota were examined, as high concentrations of TRI residues were also found in the cecum of the two groups. Principal coordinate analysis of *β*-diversity, utilizing Bray−Curtis's dissimilarity measures, disclosed a pronounced segregation among the groups (Figure 4A). This observation hints at a transformation in the composition of intestinal flora after TRI treatment. The TRI-H group displayed notably reduced Chao1 and ACE index (ANOVA; $F = 6.82$, and 6.79; $p = 0.0105$, and 0.0107) (Figure 4B, C), while the TRI-M groups exhibited significantly lower Shannon index (ANOVA; $F = 8.06$; $p = 0.0060$) (Figure 4D). The results of the *α*-diversity analyses suggest that exposure to TRI led to a decrease in the diversity of intestinal flora. In addition, Chao1 and ACE indices revealed a negative correlation between the TRI dose and gut flora diversity, with higher TRI doses reducing diversity. The Shannon index, combining species richness and evenness, may not align with TRI dose−response due to its comprehensive nature, complicating dose correlation. Qi et al. (2021) found a positive correlation between *α*-diversity and testosterone levels, which aligns well with the outcomes of the present investigation.[50] The investigation demonstrated a decrease in gut microbiota species diversity in rats after exposure to TRI, along with a reduction in testosterone levels in the gut and serum (Figure 2B, and Figure 5B). At the phylum taxonomic level, the dominant intestinal bacteria were Firmicutes (68.03% vs 72.09% vs 73.20%), Bacteroidetes (29.64% vs 24.92% vs 25.52%), Campilobacterota (1.44% vs 1.62% vs 0.28%), Proteobacteria (0.39% vs 0.59% vs 0.58%), and Actinobacteria

https://doi.org/10.1021/acs.est.4c08168
Environ. Sci. Technol. 2024, 58, 22014−22026

(0.26% vs 0.53% vs 0.24%) in the control, TRI-M, and TRI-H groups. At the genus level, exposure to TRI-treated groups significantly increased the percentage composition of *Eubacterium*, *Prevotellamassilia*, *Flavonifractor*, *Colidextribacter*, *Alistipes*, *Ihubacter*, and *Peptococcus*, while decreased the relative abundance of *Kineothrix*, *Lacrimispora*, *Eisenbergiella*, *Anaerocolumna*, *Tepidibaculum*, and *Parabacteroide* ($p < 0.05$) (Figure 4F, and Figure S6A, B). For the control group, the genera *Lacrimispora*, *Eisenbergiella*, and *Clostridium XlVa* were the main bacteria, while the genera *Eubaeterium*, *Lachnospiracea*, and *Flavonifractor* were primary in the TRI-M group (Figure S6C, D). *Butyrivibrio* and *Peptococcus* were primary in the TRI-H group (Figure S6C, D). At the same time, the number of biomarker species increased with increasing TRI doses, indicating a dose-dependent relationship.

In summary, these findings suggest that these genera could potentially function as taxonomic indicators. *Parabacteroides* play a crucial role in carbohydrate metabolism by secreting short-chain fatty acids (SCFAs) and are considered a fundamental member of the human gut microbiota.[51] *Lachnospira*, *Lacrimispora*, *Anaerobutyricum*, and *Kineothrix* are also probiotic organisms capable of producing SCFAs and secondary bile acids in the gut.[52,53] *Ihubacter* and *Lactococcus* can cause a variety of infections in humans and are a recognized genus of pathogenic bacteria.[54,55] TRI exposure decreased beneficial SCFA-producing genera and increased detrimental genera. Reduced SCFA-producing gut microbiota may trigger inflammation, hindering testicular cell development and maturation.[56]

Alterations in gut bacteria caused functional alterations. The influence of TRI on gut bacteria functionality was subsequently analyzed utilizing the KEGG repository and the enzyme classification system. KEGG pathway analysis indicated significant inhibition of steroid hormone biosynthesis, retinol metabolism, metabolism of xenobiotics by cytochrome P450, and drug metabolism-cytochrome P450 in the TRI-treatment groups (Figure S7A). TRI exposure significantly reduced enzymes involved in cholesterol metabolism, sex hormone synthesis, and SCFA metabolism, including 7α-hydroxysteroid dehydrogenase, 20β-hydroxysteroid dehydrogenase, and butyrate kinase (ANOVA; F = 19.68, 8.28, and 16.96; p = 0.0002, 0.0259, and 0.0003) (Figure S7B). Meanwhile, the relative abundances of 7α-hydroxysteroid dehydrogenase, 20β-hydroxysteroid dehydrogenase, and butyrate kinase gradually decreased with increasing TRI concentration, indicating a dose-dependent relationship. Changes in enzyme function suggest that TRI exposure disrupted SCFAs metabolism, bile acids, and steroid hormones pathways associated with gut microbiota.[57−59] Subsequently, metabolomic profiling was undertaken to gain deeper insights into the modifications of gut metabolites.

3.6. Metabolomics Analysis on the TRI-Exposed Rat Cecum Fecal. An untargeted metabolomic analysis was employed to delineate the alterations in the metabolite profile within rat cecal feces after exposure to varying doses of TRI. The counts of endogenous significantly altered metabolites (SCMs) in TRI-L, TRI-M, and TRI-H were 193 (80 downregulated and 113 upregulated), 231 (86 downregulated and 145 upregulated), and 549 (254 downregulated and 295 upregulated), respectively ($p < 0.05$, Figure S8A, B). The number of SCMs increased with increasing doses of TRI exposure, indicating a dose-dependent relationship (Figure S8B). Bile acids, such as chenodeoxycholic acid (CDCA), hyocholic acid, and CDCA-3-sulfate, exhibited a significant increase in their relative abundance (Figure S8B). Furthermore, DL-glyceric acid, a precursor for SCFAs production by intestinal microorganisms, experienced a noticeable decrease in its relative abundance (Figure S8B).

Based on all metabolites found, steroid hormone biosynthesis, steroid biosynthesis, retinol metabolism, propanoate metabolism, and primary bile acid biosynthesis pathways were enriched (Figure 5A). Furthermore, these pathways were also identified in transcriptomics analyses and predictive analyses of gut microbiota function.

The deep MetOrigin analysis focused on differential metabolites originating from bacteria, the host, or both sources. Overall, TRI exposure reduced the proportion of SCMs in steroid hormone biosynthesis, propanoate metabolism, and retinol metabolism pathways, whereas it increased the proportion of SCMs in bile acid biosynthesis pathways (Figure 5B). Meanwhile, concentrations of key metabolites such as dihydroxy pregnenolone, T, DHT, progesterone, propionic acid, retinoic acid, CDCA, hyocholic acid, and CDCA-3-sulfate in rat cecum were also relative quantified using UPLC-QE (Figure S9). Compared with the control group, notable concentration reductions were observed in T, DHT, dihydroxy pregnenolone, progesterone, propionic acid, and retinoic acid within the TRI-H samples (ANOVA; F = 6.98, 14.22, 22.83, 4.59, 6.80, and 5.52; p = 0.0042, 0.0002, 0.0001, 0.0195, 0.0047, and 0.0103) (Figure S9A-D, H, and I), while CDCA and hyocholic acid concentrations were significantly elevated in the TRI-H samples (ANOVA; F = 406.20, and 3.63; p = 0.0001, and 0.0451) (Figure S9F, G). Exposure to the TRI-M group also reduced rat cecum T, DHT, and progesterone concentrations, while CDCA concentrations were significantly increased (Figure S9A, D, and F). The results of relative quantification of target metabolites were consistent with the nontargeted metabolomics results (Figure S9J).

Metabolomic profiling of the gut showed a marked decline in steroid hormone concentrations, indicating that TRI inhibited steroid hormone biosynthesis pathway genes affecting hormone synthesis. Additionally, a decrease in the relative concentration of SCFAs results in diminished binding affinity to the olfactory receptor 51E2 (OR51E2) on the sperm surface, inhibiting sperm maturation and migration.[56] The conversion of CDCA is hindered by a decrease in 7α-hydroxysteroid dehydrogenase, increasing the relative concentration of CDCA.[60] The increase in the relative concentration of CDCA, a potent inhibitor of sterol 27-hydroxylase cytochrome P450 27A1 (CYP27A1), consequently lowers plasma cholesterol levels.[60] This may be a direct cause of the decrease in total blood cholesterol levels due to the involvement of gut microbiota after exposure to TRI. Meanwhile, a decrease in the relative abundance of retinoic acid, a key signaling molecule for spermatocyte proliferation and sperm maturation and release, also contributes to testicular damage.[61] In conclusion, TRI exposure disrupted the gut microbial ecosystem, adversely affecting the reproductive system.

3.7. Multiomics Integration Analysis. Joint analysis of KEGG-enriched pathways in the testicular transcriptome and intestinal metabolome revealed simultaneous enrichment of steroid hormone biosynthesis, retinol metabolism, and propanoate metabolism (Figure S10A).

https://doi.org/10.1021/acs.est.4c08168
Environ. Sci. Technol. 2024, 58, 22014−22026

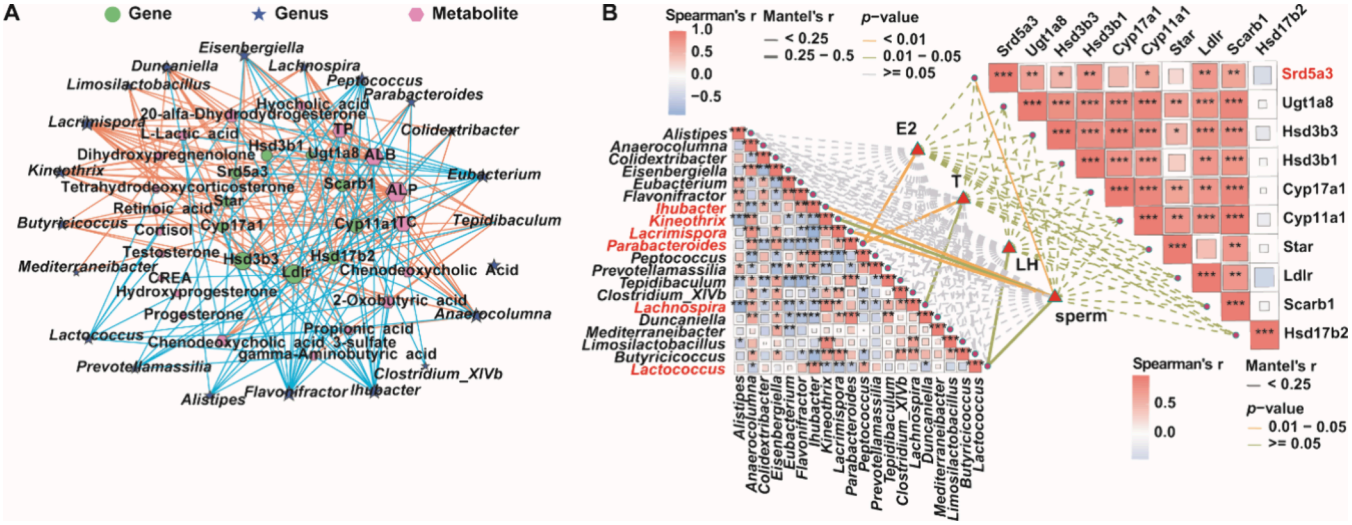

Figure 6. Multiomics integration analysis. (A) Association network diagrams for differential genera, differential metabolites, and differential genes. The graph's node size indicates the substance's connectivity, with larger nodes representing higher connectivity. The thickness of the lines in the graph corresponds to the absolute value of the correlation, with thicker lines indicating stronger correlations. The red lines indicate a significant positive correlation ($R > 0.5$ and $p < 0.05$), while the blue lines indicate a significant negative correlation ($R < -0.5$ and $p < 0.05$). (B) Pairwise comparisons of differential genus or differential genes. Serum hormone levels (including E_2, T, and LH) and sperm counts in various doses of TRI-exposed groups were analyzed for correlation with differential genes involved in Steroid hormone biosynthesis, as well as differential genera, using Mantel tests with Bonferroni correction. The color gradient denotes Spearman's correlation coefficients. Edge width corresponds to Mantel's r statistic for the corresponding distance correlations. The edge color denotes the statistical significance of Mantel's p-value. * indicated $p < 0.05$, ** indicated $p < 0.01$, and *** indicated $p < 0.001$.

Key metabolites, including testosterone, hydroxyprogesterone, calcitriol, retinoic acid, and propionic acid, whose abundance decreased, were significantly associated with *ClostridiumXlVb*, *Lachnospira*, *Mediterraneibacter*, *Limosilactobacillus*, and *Duncaniella* genera showing positive correlations (Figure S10B-E). *ClostridiumXlVb* produces indole-3-propionic acid, which is involved in cholesterol transport.[62] *Lachnospira*, *Mediterraneibacter*, and *Limosilactobacillus* are potentially beneficial bacteria that mainly produce propionic acid and butyric acid, and have anti-inflammatory activities.[63,64] Conversely, *Butyricicoccus*, *Eubacterium*, *Lactococcus*, and *Bifidobacterium* displayed a marked elevation in proportional prevalence and exhibited a pronounced negative correlation (Figure S10B-E). Network analysis of steroid hormone biosynthesis genes, differential genera, and metabolites identified *Hsd3b3*, *Ldlr*, and *Cyp11a1* as the top three genes by connectivity (Figure 6A). The downregulated genes *Hsd3b3*, *Ldlr*, and *Cyp11a1* displayed negative correlations with *Flavonifractor*, *Peptococcus*, and *Ihubacter* while showing positive correlations with *Lacrimispora*, *Anaerocolumna*, *Duncaniella*, TP, TC, ALP, and ALB (Figure 6A). *Lacrimispora* and *Anaerocolumna* both are SCFAs-producing bacterium.[65] Hyocholic acid, CDCA, and CDCA-3-sulfate, which are related to bile acid metabolism, all exhibited negative correlations with *Eisenbergiella* and *Anaerocolumna*, and positive correlations with *Colidextribacter*. *Eisenbergiella* is a pro-inflammatory microbe that increases inflammatory mediators,[66] while *Colidextribacter* is a beneficial bacterium promoting SCFAs production.[67] Additionally, these bile acids showed significant positive correlations with *Hsd17b2* (Figure 6A). In summary, TRI administration altered bacterial composition, strongly correlating with genes related to steroid hormone biosynthesis.

Overall correlation analysis demonstrated significant associations between sperm counts and *Srd5a3* gene expression, as well as abundances of *Ihubacter*, *Kineothrix*, *Lacrimispora*, and *Lactococcus* (Figure 6B). *Ihubacter* is a key microbe in the production of trimethylamine, which further induces the expression of pro-inflammatory markers and inhibits reverse cholesterol transport.[54] The study also found significant correlations between hormone levels (E_2 and T) and the relative abundance of *Parabacteroides*. Studies have shown that *Parabacteroides* has a specific effect on ameliorating testicular damage. Mice transplanted with *Parabacteroides* exhibited a significant increase in testicular weight and sperm count.[68] Additionally, T levels were significantly associated with *Lachnospira* abundance, while LH levels correlated significantly with *Lactococcus* abundance. Finally, multiomics analyses pinpointed steroid hormone biosynthesis, retinol metabolism, and propanoate metabolism pathways as crucial pathways involved in testicular damage, reduced sperm counts, and decreased sex hormone levels in male rats exposed to TRI. Upon TRI exposure, *Parabacteroides*, *Lachnospira*, *Anaerobutyricum*, *Lacrimispora*, *Kineothrix*, *Ihubacter*, and *Lactococcus* emerged as key genera influencing the reproductive system via gut microbial alterations. In conclusion, shifts in bacteria producing SCFAs significantly impact metabolites and contribute to hormonal disorders.

Based on the gut microbiome, metabolomics, and joint analysis, a predicted adverse outcome pathway (AOP) network for TRI exposure in rats was formulated (Figure S14A). AOP encompasses molecular initiation events (MIEs), key events (KEs), key event relationships (KERs), and adverse outcomes (AO). Briefly, TRI binds to the quinone oxidation (Qo) site of gut microbial Cytochrome *b*, blocking electron transfer to cytochrome C1 as MIEs.[24] This further impedes nicotinamide adenine dinucleotide (NADH) and ATP production, decreased gut microbiota diversity, reduced beneficial bacteria, diminished SCFAs and retinoic acid synthesis, increased CDCA synthesis, reduced steroid hormone synthesis raw materials, and hindered the maturation and release of

https://doi.org/10.1021/acs.est.4c08168
Environ. Sci. Technol. 2024, 58, 22014−22026

spermatozoa, which was the major KEs. Insufficient production of androgens, which compromises the structure of the seminiferous tubules, results in testicular damage. This damage subsequently leads to a decrease in the number of sperm transported to the epididymis, which is the main AO.

3.8. Effects of TRI on LNCaP Cell Proliferation and β-galactosidase Activity in Yeast. Cell proliferation tests were conducted to further verify the inhibitory effect of TRI on steroid hormone production. LNCaP cells express AR, which is a commonly used tool to identify AR active compounds based on its androgen-dependent cell proliferation.[69] LNCaP cell viability increased progressively with a gradual increase in T concentration in the culture medium (Figure S11A). After T (1.00×10^{-8} mol/L) exposure, the relative proliferation rate of LNCaP cells increased to 146.11% of the control group ($p < 0.05$) (Figure S11B). In the agonistic assay, 1.00×10^{-8} mol/L and 1.00×10^{-7} mol/L TRI exposure increased the relative proliferation rate of LNCaP cells to 128.62% and 123.74% of the control group, respectively (ANOVA; $F = 2.28$; $p = 0.0490$) (Figure S11B). In the antagonistic assay, TRI combined with T (1.00×10^{-8} mol/L) exposure to LNCaP cells reduced the relative cell proliferation rate to 55.28%−66.99% of the positive control group at all concentrations (ANOVA; $F = 7.07$; $p < 0.0001$) (Figure S11B). This result indicates that TRI may disrupt AR activity and reduce T's stimulatory effect on LNCaP cell proliferation, suggesting an antagonistic interaction between TRI and T.

The yeast two-hybrid system provides possibilities to detect both agonists as well as antagonists at the level of AR functioning.[70] The β-galactosidase activity of recombinant two-hybrid yeast increased significantly with an increasing dihydrotestosterone (DHT) concentration (Figure S11C). At all concentrations, exposure to TRI alone resulted in no significant change in the β-galactosidase activity of recombinant two-hybrid yeast compared to the control. β-galactosidase activity in recombinant two-hybrid yeast gradually decreased with an increasing TRI concentration in the presence of DHT (Figure S11D). At concentrations of 1.00×10^{-7} mol/L and 1.00×10^{-6} mol/L, TRI combined with DHT significantly decreased the β-galactosidase activity in recombinant two-hybrid yeast compared to the positive control (ANOVA; $F = 18.66$; $p < 0.0001$) (Figure S11D). *In vitro* assays show that TRI acts as an endocrine disruptor by competitively binding AR, inhibiting androgen downstream signaling and reducing cell proliferative capacity and β-galactosidase activity. Further, molecular docking analysis explored the interaction between TRI and AR. The interaction energy of TRI with rat AR (−48.75 kcal/mol) was higher than that with the positive AR inhibitor (n-aryl-oxazolidin-2-imine) (−43.85 kcal/mol) (Figure S12A, B). Ten amino acid residues within the rat AR participated in the binding interactions with n-aryl-oxazolidin-2-imine and TRI. Both n-aryl-oxazolidin-2-imine and TRI formed hydrogen bonding interactions with ARG752 and ASN705. These outcomes imply that TRI may enter the same docking pocket as inhibitors of AR. Outcomes from *in vitro* and *in silico* analysis are consistent with those of previous computational models, TRI is a potential AR antagonist.[17] The findings additionally underscored the disruptive effects of TRI on testicular function.

3.9. Molecular Docking of TRI with LDLR and SCARB1. To further elucidate the potential interactions between LDLR and SCARB1 and TRI, molecular docking analyses were performed. This is an important means to uncover MIEs.[71] The lowest binding mode of CDOCKER_INTERACTION_ENERGY is illustrated in Figure S13. Rat LDLR exhibited 56% sequence similarity to human LDLR, while rat SCARB1 displayed 61% sequence similarity to AlphaFold Model rat SCARB1 based on homologous modeling. In addition, agisterol and ITX5061, which are antagonists of LDLR and SCARB1, were selected as natural ligands for comparison. The interaction energy of TRI with rat LDLR (−57.13 kcal/mol) was higher than with agisterol (−46.76 kcal/mol) (Figure S13A, B). Twenty-five amino acid residues within the rat LDLR participated in the binding interactions with agisterol and TRI. Both agisterol and TRI formed hydrogen bonding interactions with ILE522. Furthermore, TRI exhibited an interaction energy similar to that of rat SCARB1 (−48.23 kcal/mol) compared to that of ITX5061 (−46.93 kcal/mol) (Figure S13C, D). Twenty-one amino acid residues of rat SCARB1 are involved in binding with ITX5061 and TRI. Both ITX5061 and TRI form hydrogen bonding interactions with ARG98. In addition, the docking of TRI to both LDLR and SCARB1 formed more hydrogen bonds in comparison to the natural ligands. These outcomes imply that TRI may enter the same docking pocket as inhibitors of LDLR and SCARB1.

Molecular docking results revealed that TRI accessed the same binding pockets with higher interaction energies and more hydrogen bonding than the two cholesterol receptor inhibitors. A predicted AOP network for TRI exposure in rats was formulated based on the aforementioned findings (Figure S14B). In summary, TRI exposure is predicted to inhibit LDLR and SCARB1 activity and serves as MIEs. Reduced LDLR and SCARB1 activity impaired cholesterol absorption and transport in Leydig cells, decreasing testosterone production and inhibiting the AR signaling pathway, leading to seminiferous tubule structural alterations and testicular injury, which were the main KEs. Testicular damage further decreased the number of sperm transported to the epididymis, which is the main AO.

In conclusion, this study is the first to find TRI as a cholesterol receptor antagonist that induces reproductive toxicity in male rats. In addition, TRI-induced gut microbiota dysbiosis interferes with the synthesis of CDCA, SCFA, retinoic acid, and steroid hormones, leading to testicular damage in male rats. In this study, our main purpose is to stress the sensitivity and effectiveness of multi omics joint analysis in exploring molecular mechanisms of TRI. There is a need to further study the key gut microbiota at the species level and to reveal their mechanisms as biomarkers of reproductive diseases. Furthermore, additional knockout, single-bacteria screening, and drug-assisted validation experiments are required to validate the predicted network of AOPs in subsequent studies.

■ ASSOCIATED CONTENT

Supporting Information

The Supporting Information is available free of charge at https://pubs.acs.org/doi/10.1021/acs.est.4c08168.

Detailed information on experimental sections (Text S1−S11). The recovery rate of TRI in rat tissues and serum (Table S1). The instrument parameters of HPLC-MS-MS for TRI (Table S2). The selective reaction monitor (SRM) parameters for TRI, testosterone and progesterone (Table S3). The recovery rate of

https://doi.org/10.1021/acs.est.4c08168
Environ. Sci. Technol. 2024, 58, 22014−22026

testosterone and progesterone in serum (Table S4). The instrument parameters of HPLC-MS-MS for testosterone and progesterone (Table S5). The name and primer sequences used for real-time PCR analysis (Table S6). The instrument parameters for metabolomic analysis (Table S7). The precursor ion and product ions of several metabolites used for relative quantification on UPLC-QE (Table S8). The TRI concentration in rat tissues and serum after different TRI exposures (Figure S1). Effects of TRI exposure on body weight in SD rats (Figure S2). Effects of TRI exposure on serum biochemistry in SD rats (Figure S3). Transcriptomic analysis on the TRI-exposed rat testis (Figure S4). RT-qPCR analysis on the TRI-exposed rat testis (Figure S5). Effects of TRI exposure on gut microbiota composition and function of rats (Figure S6, 7); Metabolomics analysis on the TRI-exposed rat cecum fecal (Figure S8). Relative quantification of target metabolites analysis on the TRI-exposed rat cecum faecal (Figure S9). Multiomics integration analysis (Figure S10). Effects of TRI exposure on LNCaP cell proliferation and DHT-induced β-galactosidase activity in yeast (Figure S11). Molecular docking analysis (Figure S12, 13). Predicted adverse outcome pathways (AOP) network of TRI with rat model (Figure S14) (PDF)

AUTHOR INFORMATION

Corresponding Authors

Jing Chang − *Research Center for Eco-Environmental Sciences, Chinese Academy of Sciences, Beijing 100085, China;* orcid.org/0000-0001-7366-8317; Email: jingchang@rcees.ac.cn

Huili Wang − *Research Center for Eco-Environmental Sciences, Chinese Academy of Sciences, Beijing 100085, China;* orcid.org/0000-0002-0984-2963; Email: huiliwang@rcees.ac.cn

Authors

Zheng Ma − *Research Center for Eco-Environmental Sciences, Chinese Academy of Sciences, Beijing 100085, China; University of Chinese Academy of Sciences, Beijing 100049, China*

Jianzhong Li − *Research Center for Eco-Environmental Sciences, Chinese Academy of Sciences, Beijing 100085, China*

Bin Wan − *Research Center for Eco-Environmental Sciences, Chinese Academy of Sciences, Beijing 100085, China; University of Chinese Academy of Sciences, Beijing 100049, China;* orcid.org/0000-0002-3339-577X

Complete contact information is available at: https://pubs.acs.org/10.1021/acs.est.4c08168

Author Contributions

Z.M.: investigation, data curation, writing - original draft and editing. J.C.: supervision, resources, wqriting - review and editing, project administration, funding acquisition. J.L.: supervision. B.W.: writing - review and editing, supervision. H.W.: methodology, writing - review and editing, supervision.

Notes

The authors declare no competing financial interest.

ACKNOWLEDGMENTS

The authors appreciate the assistance from colleagues at the Research Center for Eco-Environmental Sciences, Chinese Academy of Sciences, particularly Professor Ma Mei and Associate Professor Li Na, for providing recombinant androgen receptor gene two-hybrid yeast and for their valuable guidance on relevant methodologies. The work was supported by the National Natural Science Foundation of China (Grant numbers: 42207320, 22076214).

REFERENCES

(1) Jia, L.; Huang, X.; Zhao, W.; Wang, H.; Jing, X. An effervescence tablet-assisted microextraction based on the solidification of deep eutectic solvents for the determination of strobilurin fungicides in water, juice, wine, and vinegar samples by HPLC. *Food Chem.* **2020**, *317*, No. 126424.

(2) Qu, H.; Zhao, Y.; Du, S.; Li, P.; Wu, S. Role of solvent properties and composition on the solid-liquid equilibrium of trifloxystrobin and thermodynamic analysis. *J. Mol. Liq.* **2019**, *294*, No. 111566.

(3) Chen, L.; Luo, Y.; Zhang, C.; Liu, X.; Fang, N.; Wang, X.; Zhao, X.; Jiang, J. Trifloxystrobin induced developmental toxicity by disturbing the ABC transporters, carbohydrate and lipid metabolism in adult zebrafish. *Chemosphere* **2024**, *349*, No. 140747.

(4) Ernst, F.; Alonso, B.; Colazzo, M.; Pareja, L.; Cesio, V.; Pereira, A.; Márquez, A.; Errico, E.; Segura, A. M.; Heinzen, H. Occurrence of pesticide residues in fish from south American rainfed agro-ecosystems. *Sci. Total Environ.* **2018**, *631*, 169−179.

(5) Saha, A.; Makwana, C.; Meena, R. P.; Manivel, P. Residual dynamics of azoxystrobin and combination formulation of trifloxystrobin 25%+ tebuconazole 50%-75 W G on isabgol (*Plantago ovata Forssk.*) and soil. *J. Appl. Res. Med. Aromat. Plants* **2020**, *17*, No. 100227.

(6) Shang, N.; Yang, Y.; Xiao, Y.; Wu, Y.; Li, K.; Jiang, X.; Sanganyado, E.; Zhang, Q.; Xia, X. Exposure levels and health implications of fungicides, neonicotinoid insecticides, triazine herbicides and their associated metabolites in pregnant women and men. *Environ. Pollut.* **2024**, *342*, No. 123069.

(7) Shanmugam, P. S. T.; Sampath, T.; Jagadeeswaran, I.; Thamizharasan, S.; Fathima, S. Reproduction toxicity. *In Biocompatibility Protocols for Medical Devices and Materials* **2023**, 159−173.

(8) Liu, T.; Liu, Y.; Fang, K.; Zhang, X.; Wang, X. Transcriptome, bioaccumulation and toxicity analyses of earthworms (*Eisenia fetida*) affected by trifloxystrobin and trifloxystrobin acid. *Environ. Pollut.* **2020**, *265*, No. 115100.

(9) Li, H.; Cao, F.; Zhao, F.; Yang, Y.; Teng, M.; Wang, C.; Qiu, L. Developmental toxicity, oxidative stress and immunotoxicity induced by three strobilurins (pyraclostrobin, trifloxystrobin and picoxystrobin) in zebrafish embryos. *Chemosphere* **2018**, *207*, 781−790.

(10) Cui, F.; Chai, T.; Liu, X.; Wang, C. Toxicity of three strobilurins (kresoxim-methyl, pyraclostrobin, and trifloxystrobin) on *Daphnia magna*. *Environ. Toxicol. Chem.* **2017**, *36* (1), 182−189.

(11) Zhu, L.; Wang, H.; Liu, H.; Li, W. Effect of trifloxystrobin on hatching, survival, and gene expression of endocrine biomarkers in early life stages of medaka (*Oryzias latipes*). *Environ. Toxicol.* **2015**, *30* (6), 648−655.

(12) Zhu, B.; Liu, G. L.; Liu, L.; Ling, F.; Wang, G. X. Assessment of trifloxystrobin uptake kinetics, developmental toxicity and mRNA expression in rare minnow embryos. *Chemosphere* **2015**, *120*, 447−455.

(13) Cao, F.; Martyniuk, C. J.; Wu, P.; Zhao, F.; Pang, S.; Wang, C.; Qiu, L. Long-term exposure to environmental concentrations of azoxystrobin delays sexual development and alters reproduction in zebrafish (*Danio rerio*). *Environ. Sci. Technol.* **2019**, *53* (3), 1672−1679.

(14) Kovacevic, M.; Hackenberger, D. K.; Hackenberger, B. K. Effects of strobilurin fungicides (azoxystrobin, pyraclostrobin, and

trifloxystrobin) on survival, reproduction and hatching success of *enchytraeus crypticus*. *Sci. Total Environ.* **2021**, *790*, No. 148143.
(15) Arena, M.; Auteri, D.; Barmaz, S.; Bellisai, G.; Brancato, A.; Brocca, D.; Bura, L.; Byers, H.; Chiusolo, A.; Court Marques, D.; Crivellente, F.; De Lentdecker, C.; De Maglie, M.; Egsmose, M.; Erdos, Z.; Fait, G.; Ferreira, L.; Goumenou, M.; Greco, L.; Ippolito, A.; Istace, F.; Janossy, J.; Jarrah, S.; Kardassi, D.; Leuschner, R.; Lythgo, C.; Magrans, J. O.; Medina, P.; Miron, I.; Molnar, T.; Nougadere, A.; Padovani, L.; Parra Morte, J. M.; Pedersen, R.; Reich, H.; Sacchi, A.; Santos, M.; Serafimova, R.; Sharp, R.; Stanek, A.; Streissl, F.; Sturma, J.; Szentes, C.; Tarazona, J.; Terron, A.; Theobald, A.; Vagenende, B.; Verani, A.; Villamar-Bouza, L. Peer review of the pesticide risk assessment of the active substance trifloxystrobin. *EFSA Journal* **2017**, *15* (10), No. e04989.
(16) Yang, L.; Huang, T.; Li, R.; Souders, C. L.; Rheingold, S.; Tischuk, C.; Li, N.; Zhou, B.; Martyniuk, C. J. Evaluation and comparison of the mitochondrial and developmental toxicity of three strobilurins in zebrafish embryo/larvae. *Environ. Pollut.* **2021**, *270*, No. 116277.
(17) Judson, R.; Houck, K.; Paul Friedman, K.; Brown, J.; Browne, P.; Johnston, P. A.; Close, D. A.; Mansouri, K.; Kleinstreuer, N. Selecting a minimal set of androgen receptor assays for screening chemicals. *Regul. Toxicol. Pharmacol.* **2020**, *117*, No. 104764.
(18) Meng, Z.; Yan, Z.; Sun, W.; Bao, X.; Feng, W.; Gu, Y.; Tian, S.; Wang, J.; Chen, X.; Zhu, W. Azoxystrobin disrupts colonic barrier function in mice via metabolic disorders mediated by gut microbiota. *J. Agric. Food Chem.* **2023**, *71* (1), 789−801.
(19) Liu, J.; Chen, K.; Li, Z.; Wang, Z.; Wang, L. Glyphosate-induced gut microbiota dysbiosis facilitates male reproductive toxicity in rats. *Sci. Total Environ.* **2022**, *805*, No. 150368.
(20) Thompson, K. N.; Oulhote, Y.; Weihe, P.; Wilkinson, J. E.; Ma, S.; Zhong, H.; Li, J.; Kristiansen, K.; Huttenhower, C.; Grandjean, P. Effects of lifetime exposures to environmental contaminants on the adult gut microbiome. *Environ. Sci. Technol.* **2022**, *56* (23), 16985−16995.
(21) Valeria, C.; Virginia, R.; Giulia, M.; Corrado, R.; Chiara, H.; Simona, P.; Claudio, B.; Gianvincenzo, Z. Precocious puberty and microbiota: The role of the sex hormone−gut microbiome axis? *Front. Endocrinol.* **2022**, *13*, No. 1000919.
(22) Li, X.; Cheng, W.; Shang, H.; Wei, H.; Deng, C. The Interplay between androgen and gut microbiota: Is there a microbiota-gut-testis axis. *Reprod Sci.* **2022**, *29* (6), 1674−1684.
(23) Collden, H.; Landin, A.; Wallenius, V.; Elebring, E.; Fandriks, L.; Nilsson, M. E.; Ryberg, H.; Poutanen, M.; Sjogren, K.; Vandenput, L.; Ohlsson, C. The gut microbiota is a major regulator of androgen metabolism in intestinal contents. *Am. J. Physiol. Endocrinol. Metab.* **2019**, *317* (6), E1182−E1192.
(24) Pandey, G.; Rathore, H. Toxicity of strobilurins fungicides: A comprehensive review. *J.Chem.Health Risks* **2023**, *13*, 207−218.
(25) OECD, *Test No. 408: Repeated dose 90-day oral toxicity study in rodents*. 2018.
(26) Srivastava, N.; Pande, M. *Protocols in Semen Biology (Comparing Assays)*.; Springer, Singapore, p 0.
(27) da Cunha de Medeiros, P.; Samelo, R. R.; Silva, A. P. G.; da Silva Araujo Santiago, M.; Duarte, F. A.; de Castro, Í. B.; Perobelli, J. E. Prepubertal exposure to low doses of sodium arsenite impairs spermatogenesis and epididymal histophysiology in rats. *Environ. Toxicol.* **2019**, *34* (1), 83−91.
(28) Zhang, R.; Zhai, Q.; Yu, Y.; Li, X.; Zhang, F.; Hou, Z.; Cao, Y.; Feng, J.; Xue, P. Safety assessment of crude saponins from *Chenopodium quinoa willd.* husks: 90-day oral toxicity and gut microbiota & metabonomics study in rats. *Food Chem.* **2022**, *375*, No. 131655.
(29) Chang, J.; Jiao, M.; Zhang, Z.; Liu, W.; Li, W.; Xu, P.; Wan, B. Mechanistic insight into the adverse outcome of tire wear and road particle leachate exposure in zebrafish (*Danio rerio*) larvae. *Environ. Int.* **2023**, *178*, No. 108053.
(30) Liu, R.; Cai, D.; Li, X.; Liu, B.; Chen, J.; Jiang, X.; Li, H.; Li, Z.; Teerds, K.; Sun, J.; Bai, W.; Jin, Y. Effects of bisphenol A on reproductive toxicity and gut microbiota dysbiosis in male rats. *Ecotoxicol. Environ. Saf.* **2022**, *239*, No. 113623.
(31) Liang, J.; Yang, X.; Liu, Q. S.; Sun, Z.; Ren, Z.; Wang, X.; Zhang, Q.; Ren, X.; Liu, X.; Zhou, Q.; Jiang, G. Assessment of thyroid endocrine disruption effects of parabens using In vivo, In vitro, and In silico approaches. *Environ. Sci. Technol.* **2022**, *56* (1), 460−469.
(32) Xin, Y.; Ren, X.-M.; Wan, B.; Guo, L.-H. Comparative in vitro and in vivo evaluation of the estrogenic effect of hexafluoropropylene oxide homologues. *Environ. Sci. Technol.* **2019**, *53* (14), 8371−8380.
(33) Li, J.; Ma, M.; Wang, Z. J. A two-hybrid yeast assay to quantify the effects of xenobiotics on thyroid hormone-mediated gene expression. *Environ. Toxicol. Chem.* **2008**, *27* (1), 159−167.
(34) Waterhouse, A.; Bertoni, M.; Bienert, S.; Studer, G.; Tauriello, G.; Gumienny, R.; Heer, F. T.; de Beer, T. A P.; Rempfer, C.; Bordoli, L.; Lepore, R.; Schwede, T. SWISS-MODEL: homology modelling of protein structures and complexes. *Nucleic Acids Res.* **2018**, *46* (W1), W296−W303.
(35) Wambaugh, J. F.; Wetmore, B. A.; Ring, C. L.; Nicolas, C. I.; Pearce, R. G.; Honda, G. S.; Dinallo, R.; Angus, D.; Gilbert, J.; Sierra, T.; Badrinarayanan, A.; Snodgrass, B.; Brockman, A.; Strock, C.; Setzer, R. W.; Thomas, R. S. Assessing toxicokinetic uncertainty and variability in risk prioritization. *Toxicol. Sci.* **2019**, *172* (2), 235−251.
(36) Xiong, G.; Wu, Z.; Yi, J.; Fu, L.; Yang, Z.; Hsieh, C.; Yin, M.; Zeng, X.; Wu, C.; Lu, A.; Chen, X.; Hou, T.; Cao, D. ADMETlab 2.0: an integrated online platform for accurate and comprehensive predictions of ADMET properties. *Nucleic Acids Res.* **2021**, *49* (W1), W5−W14.
(37) Lahimer, M.; Abou Diwan, M.; Montjean, D.; Cabry, R.; Bach, V.; Ajina, M.; Ben Ali, H.; Benkhalifa, M.; Khorsi-Cauet, H. Endocrine disrupting chemicals and male fertility: from physiological to molecular effects. *Frontiers in Public Health* **2023**, *11*, No. 1232646.
(38) Vandenberg, L. N.; Welshons, W. V.; Vom Saal, F. S.; Toutain, P.-L.; Myers, J. P. Should oral gavage be abandoned in toxicity testing of endocrine disruptors? *Environ. Health* **2014**, *13*, 1−7.
(39) Liu, J.; Li, X.; Zhou, G.; Zhang, Y.; Sang, Y.; Wang, J.; Li, Y.; Ge, W.; Sun, Z.; Zhou, X. Silica nanoparticles inhibiting the differentiation of round spermatid and chromatin remodeling of haploid period via MIWI in mice. *Environ. Pollut.* **2021**, *284*, No. 117446.
(40) Zhao, T.-X.; Wei, Y.-X.; Wang, J.-K.; Han, L.-D.; Sun, M.; Wu, Y.-H.; Shen, L.-J.; Long, C.-L.; Wu, S.-D.; Wei, G.-H. The gut-microbiota-testis axis mediated by the activation of the Nrf2 antioxidant pathway is related to prepuberal steroidogenesis disorders induced by di-(2-ethylhexyl) phthalate. *Environ. Sci. Pollut. Res.* **2020**, *27* (28), 35261−35271.
(41) Spaziani, M.; Tarantino, C.; Tahani, N.; Gianfrilli, D.; Sbardella, E.; Lenzi, A.; Radicioni, A. F. Hypothalamo-pituitary axis and puberty. *Mol. Cell. Endocrinol.* **2021**, *520*, No. 111094.
(42) Płaczkowska, S.; Rodak, K.; Kmieciak, A.; Gilowska, I.; Kratz, E. M. Exploring correlations: Human seminal plasma and blood serum biochemistry in relation to semen quality. *PLoS One* **2024**, *19* (6), No. e0305861.
(43) Luo, J.; Yang, H.; Song, B.-L. Mechanisms and regulation of cholesterol homeostasis. *Nat. Rev. Mol. Cell Biol.* **2020**, *21* (4), 225−245.
(44) Schiffer, L.; Barnard, L.; Baranowski, E. S.; Gilligan, L. C.; Taylor, A. E.; Arlt, W.; Shackleton, C. H. L.; Storbeck, K.-H. Human steroid biosynthesis, metabolism and excretion are differentially reflected by serum and urine steroid metabolomes: A comprehensive review. *J. Steroid Biochem. Mol. Biol.* **2019**, *194*, No. 105439.
(45) Ma, Y.; Liu, H.; Du, X.; Shi, Z.; Liu, X.; Wang, R.; Zhang, S.; Tian, Z.; Shi, L.; Guo, H.; Zhang, H. Advances in the toxicology research of microcystins based on omics approaches. *Environ. Int.* **2021**, *154*, No. 106661.
(46) Acconcia, F.; Marino, M. Steroid hormones: synthesis, secretion, and transport. *In Principles of Endocrinology and Hormone Action* **2018**, 43−72.

https://doi.org/10.1021/acs.est.4c08168
Environ. Sci. Technol. 2024, 58, 22014−22026

(47) Chang, T.-Y.; Chang, C. C. Y.; Ohgami, N.; Yamauchi, Y. Cholesterol sensing, trafficking, and esterification. *Annu. Rev. Cell Dev. Biol.* **2006**, *22* (1), 129−157.
(48) Miller, W. L.; Auchus, R. J. The Molecular biology, biochemistry, and physiology of human steroidogenesis and its disorders. *Endocr. Rev.* **2011**, *32* (1), 81−151.
(49) Argaw-Denboba, A.; Schmidt, T. S. B.; Di Giacomo, M.; Ranjan, B.; Devendran, S.; Mastrorilli, E.; Lloyd, C. T.; Pugliese, D.; Paribeni, V.; Dabin, J.; Pisaniello, A.; Espinola, S.; Crevenna, A.; Ghosh, S.; Humphreys, N.; Boruc, O.; Sarkies, P.; Zimmermann, M.; Bork, P.; Hackett, J. A. Paternal microbiome perturbations impact offspring fitness. *Nature* **2024**, *629* (8012), 652−659.
(50) Qi, X.; Yun, C.; Pang, Y.; Qiao, J. The impact of the gut microbiota on the reproductive and metabolic endocrine system. *Gut Microbes* **2021**, *13* (1), 1−21.
(51) Cui, Y.; Zhang, L.; Wang, X.; Yi, Y.; Shan, Y.; Liu, B.; Zhou, Y.; Lü, X. Roles of intestinal *Parabacteroides* in human health and diseases. *FEMS Microbiol. Lett.* **2022**, *369* (1), No. fnac072.
(52) Vacca, M.; Celano, G.; Calabrese, F. M.; Portincasa, P.; Gobbetti, M.; De Angelis, M. The Controversial role of human gut *Lachnospiraceae*. *Microorganisms* **2020**, *8* (4), 573.
(53) Qiao, S.; Bao, L.; Wang, K.; Sun, S.; Liao, M.; Liu, C.; Zhou, N.; Ma, K.; Zhang, Y.; Chen, Y.; Liu, S.-J.; Liu, H. Activation of a specific gut bacteroides-folate-liver axis benefits for the alleviation of nonalcoholic hepatic steatosis. *Cell Rep.* **2020**, *32* (6), No. 108005.
(54) Goel, A.; Kim, B.-J.; Ncho, C.-M.; Jeong, C.-M.; Gupta, V.; Jung, J.-Y.; Ha, S.-Y.; Lee, D.-H.; Yang, J.-K.; Choi, Y.-H. Dietary supplementation of shredded, steam-exploded pine particles decreases pathogenic microbes in the cecum of acute heat-stressed broilers. *Animals* **2021**, *11* (8), 2252.
(55) Jung, M. Y.; Lee, C.; Seo, M.-J.; Roh, S. W.; Lee, S. H. Characterization of a potential probiotic bacterium *Lactococcus raffinolactis WiKim0068* isolated from fermented vegetable using genomic and in vitro analyses. *BMC Microbiol.* **2020**, *20* (1), 136.
(56) Teveroni, E.; Di Nicuolo, F.; Vergani, E.; Bruno, C.; Maulucci, G.; Bianchetti, G.; Astorri, A. L.; Grande, G.; Gervasoni, J.; Santucci, L.; De Spirito, M.; Urbani, A.; Pontecorvi, A.; Mancini, F.; Milardi, D. Short-chain fatty acids modulate sperm migration through olfactory receptor 51E2 activity. *Int. J. Mol. Sci.* **2022**, *23* (21), 12726.
(57) Tanaka, N.; Nonaka, T.; Tanabe, T.; Yoshimoto, T.; Tsuru, D.; Mitsui, Y. Crystal structures of the binary and ternary complexes of 7α-hydroxysteroid dehydrogenase from Escherichia coli. *Biochemistry* **1996**, *35* (24), 7715−7730.
(58) Doden, H. L.; Pollet, R. M.; Mythen, S. M.; Wawrzak, Z.; Devendran, S.; Cann, I.; Koropatkin, N. M.; Ridlon, J. M. Structural and biochemical characterization of 20β-hydroxysteroid dehydrogenase from *Bifidobacterium adolescentis* strain L2−32. *J. Biol. Chem.* **2019**, *294* (32), 12040−12053.
(59) Louis, P.; Duncan, S. H.; McCrae, S. I.; Millar, J.; Jackson, M. S.; Flint, H. J. Restricted distribution of the butyrate kinase pathway among butyrate-producing bacteria from the human colon. *J. Bacteriol.* **2004**, *186* (7), 2099−2106.
(60) Fiorucci, S.; Distrutti, E. *Bile acids and their receptors.*; Springer, Cham, p 0.
(61) Zhang, H. Z.; Hao, S. L.; Yang, W. X. How does retinoic acid (RA) signaling pathway regulate spermatogenesis? *Histol. Histopathol.* **2022**, *37* (11), 1053−1064.
(62) Xue, H.; Chen, X.; Yu, C.; Deng, Y.; Zhang, Y.; Chen, S.; Chen, X.; Chen, K.; Yang, Y.; Ling, W. Gut microbially produced indole-3-propionic acid inhibits atherosclerosis by promoting reverse cholesterol transport and its deficiency is causally related to atherosclerotic cardiovascular disease. *Circ. Res.* **2022**, *131* (5), 404−420.
(63) Abdugheni, R.; Wang, W. Z.; Wang, Y. J.; Du, M. X.; Liu, F. L.; Zhou, N.; Jiang, C. Y.; Wang, C. Y.; Wu, L.; Ma, J.; Liu, C.; Liu, S. J. Metabolite profiling of human-originated *Lachnospiraceae* at the strain level. *iMeta* **2022**, *1* (4), No. e58.
(64) Abuqwider, J.; Altamimi, M.; Mauriello, G. *Limosilactobacillus reuteri* in health and disease. *Microorganisms* **2022**, *10* (3), 522.
(65) Ueki, A.; Kaku, N.; Ueki, K. Anaerotaenia. *In Bergey's Manual of Systematics of Archaea and Bacteria* **2019**, 1−7.
(66) Saqib, Z.; De Palma, G.; Lu, J.; Surette, M.; Bercik, P.; Collins, S. M. Alterations in fecal β-defensin-3 secretion as a marker of instability of the gut microbiota. *Gut Microbes* **2023**, *15* (1), 2233679.
(67) Liu, X.; Zhang, Y.; Li, W.; Zhang, B.; Yin, J.; Liuqi, S.; Wang, J.; Peng, B.; Wang, S. Fucoidan ameliorated dextran sulfate sodium-induced ulcerative colitis by modulating gut microbiota and bile acid metabolism. *J. Agric. Food Chem.* **2022**, *70* (47), 14864−14876.
(68) Zhao, Q.; Huang, J.-F.; Cheng, Y.; Dai, M.-Y.; Zhu, W.-F.; Yang, X.-W.; Gonzalez, F. J.; Li, F. Polyamine metabolism links gut microbiota and testicular dysfunction. *Microbiome* **2021**, *9* (1), 224.
(69) Abate-Shen, C.; Nunes de Almeida, F. Establishment of the LNCaP cell line - The dawn of an era for prostate cancer research. *Cancer Res.* **2022**, *82* (9), 1689−1691.
(70) La Merrill, M. A.; Vandenberg, L. N.; Smith, M. T.; Goodson, W.; Browne, P.; Patisaul, H. B.; Guyton, K. Z.; Kortenkamp, A.; Cogliano, V. J.; Woodruff, T. J.; Rieswijk, L.; Sone, H.; Korach, K. S.; Gore, A. C.; Zeise, L.; Zoeller, R. T. Consensus on the key characteristics of endocrine-disrupting chemicals as a basis for hazard identification. *Nature Reviews Endocrinology* **2020**, *16* (1), 45−57.
(71) Montes-Grajales, D.; Morelos-Cortes, X.; Olivero-Verbel, J. Discovery of new protein targets of BPA analogs and derivatives associated with noncommunicable diseases: A virtual high-throughput screening. *Environ. Health Perspect.* **2021**, *129* (3), 37009.

https://doi.org/10.1021/acs.est.4c08168
Environ. Sci. Technol. 2024, 58, 22014−22026